Journal of Alloys and Compounds 507 (2010) 93–96

Contents lists available at ScienceDirect

Journal of Alloys and Compounds

journal homepage: www.elsevier.com/locate/jallcom

Synthesis and dislocations of 1111-type GdFePO superconductor

C.Y. Liang[b], R.C. Che[a,b,*], F. Xia[a,b], X.L. Zhang[b], H. Cao[b], Q.S. Wu[b]

[a] Department of Material Science, Fudan University, Shanghai 200438, China
[b] Department of Chemistry and Laboratory of Advanced Materials, Fudan University, Shanghai 200438, China

ARTICLE INFO

Article history:
Received 15 May 2010
Received in revised form 9 July 2010
Accepted 9 July 2010
Available online 16 July 2010

Keywords:
Superconductor
Transmission electron microscopy
Dislocation
Solid state reaction

ABSTRACT

Pnictide oxide superconductor GdFePO has been synthesized by a two-step solid reaction method. Gd–Fe–P ternary alloy is firstly prepared using pre-melting technology. The superconductivity at around 6.1 K in GdFePO is observed. An annealing treatment done after synthesis could effectively reduce the dislocation density and furthermore affect the superconducting transition. Detail evidences based on transmission electron microscopy analysis reveal the relationship between the adjustable superconducting properties and the dislocations along [0 0 1] orientation of GdFePO.

1. Introduction

The discovery of superconductivity at T_c's up to 26 K in iron arsenide compounds has stimulated the search for new superconductors with similar phase structures [1]. These groups of superconducting materials include LiFeAs, $AEFe_2As_2$ (AE = alkaline earth metals), *RE*Fe*Pn*O (abbreviated as 1111; *RE* = rare earth elements; *Pn* = pnictide elements), AEFeAsF and chalcogenide materials [2–8]. Previously, the vast majority of the reported works focused on arsenic-based compounds since, thus far, they hold the current highest T_c values (>50 K). In contrast, data about phosphor-based versions of these compounds is still in lack. The problem about superconductivity origin in both two types of materials still remains unclear. *RE*FeAsO itself are not superconducting without dopant elements, but show an anomaly transition at ~150 K in the curves of temperature dependency on both resistivity and magnetic susceptibility [9].

Recently, superconductivity was found from PrFePO and NdFePO at T_c around 3 K. Oxygen annealing has effect on chemical homogeneity and T_c was accordingly increased [10]. Measurements of Fermi surface with de Haas–van Alphen oscillations in LaFePO material showed a dominant interband scattering and a shrinking of the Fermi pockets [11–12]. In particular, transition from *P*4/*nmm* to *Cmma* was observed from FeSe superconductor [15]. $La_{1-x}FePO$ ($0 \le x \le 0.2$) with hole doped superconductivity was successfully prepared in a vacuum at 1373 K [16]. Iron selenide and telluride were synthesized through a solid state reaction at 450–550 °C [17]. Moreover, superconductivity could be induced by fluorine doping, which lead to an antiferromagnetic spin density wave (SDW) instability and a Fermi surface nesting. Mn doping can depress the superconductivity transition temperature in $Ba_{0.5}K_{0.5}Fe_2As_2$ via pair-breaking effects [18].

Nevertheless, there is no consensus on the superconducting mechanism governing FeP system of superconductors. In our previous study, high quality LaFePO superconductor was synthesized by a two-step solid reaction method [13]. In the present paper, as a new member of *RE*Fe*Pn*O family, GdFePO is fabricated through a similar routine as Ref. [13]. Superconductivity of GdFePO can be tuned by an annealing done after synthesis under oxygen atmosphere. Transmission electron microscopy (TEM) observation shows that the dislocation defects along the *c* orientation have influences on the superconducting properties. Our results might shed new light on the understanding of FeP based superconductors from the structural point of view.

2. Experimental

2.1. Synthesis

GdFePO polycrystalline sample used in this study was synthesized by a method similar to Ref. [13]. To study how the post-annealing treatment under a low oxygen atmosphere influences the superconductivity of GdFePO, the as-made pellet was divided into two equal portions and was put into two quartz tubes, respectively. A small amount of Gd_2O_3 powder was added into one of the tubes, but not into the other tube. Purpose of the added Gd_2O_3 powder was to introduce a little oxygen gas for the post-annealing treatment. The sintering temperature ~1200 °C and time were the same as used for the first time.

* Corresponding author at: Department of Chemistry and Laboratory of Advanced Materials, Fudan University, SongHu Road No. 2205, Shanghai 200438, China.
E-mail address: rcche@fudan.edu.cn (R.C. Che).

0925-8388/$ – see front matter © 2010 Elsevier B.V. All rights reserved.
doi:10.1016/j.jallcom.2010.07.090

2.2. Characterization

X-ray diffraction (XRD) for the structure determination was performed at room temperature on a Rigaku RINT X-ray diffractometer with Cu-K radiation. Temperature dependence of magnetization and resistivity were measured using an Oxford multiparameter measurement system (Maglab-Exa-12). Resistivity of superconducting samples was measured by a standard four-point probe technique. A JEM-2100F transmission electron microscope (TEM) equipped with a post-column Gatan imaging filter (GIF-Tridium) was used for TEM imaging.

3. Results and discussion

Fig. 1(a) shows an experimental XRD pattern obtained from the as-prepared GdFePO sample. All the diffraction peaks could be well indexed by a tetragonal GdFePO cell with lattice parameters of $a = 3.859$ Å, $c = 8.132$ Å and a space group of $P4/nmm$. A calculated XRD profile is shown in Fig. 1(b). This theoretical XRD simulation has been performed using the reflection computer code implemented in Cerius[2] software. Structural model used for the simulation is shown in the inset of Fig. 1(b), which illustrates a brief structural model of GdFePO crystal and is similar to that of the well-known LaFePO crystal. Each primitive cell includes eight atoms inside two sub-units. The simulated XRD profile as illustrated in Fig. 1(b) show up the main structural features in good agreement with the experimental data. Fig. 1(c) is a low-magnification SEM image of the as-sintered GdFePO product, clearly showing the layered-structural feature of the crystalline grain in a superconducting material. Thin pieces with a thickness of about 10 nm can be frequently observed. It is evident that the layered GdFePO phase is quite pure in the sample and the crystalline quality is high.

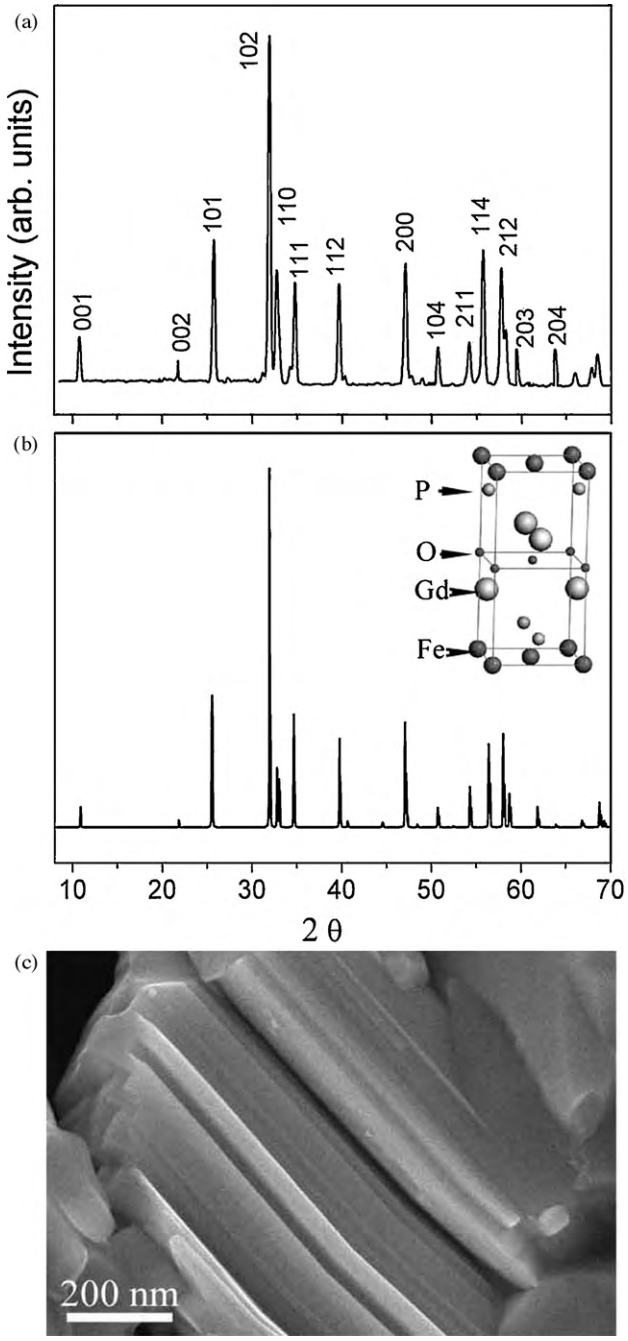

Fig. 1. (a) Powder X-ray diffraction (XRD) patterns recorded from the as-synthesized product. (b) A calculated XRD profile for GdFePO crystal, using Cerius[2] software. Inset: an atomic model of GdFePO crystal (space group $p4/nmm$, $a = 3.86$ Å and $c = 8.13$ Å). (c) Low-magnification SEM image of the GdFePO sample.

It should be noted that the experimental conditions and synthesis parameters used in the solid powder calcination play critical roles in the formation of GdFePO superconducting phase. Our previous work indicates that the annealing under low oxygen pressure done after synthesis favors the appearance of superconductivity in LaFePO, which is confirmed by the changes of Fe $L_{2,3}$ and O K excitation edges in the electron energy loss spectroscopy (EELS) data [14].

Fig. 2(a) displays the magnetic susceptibility curves for the GdFePO samples before and after the post-annealing treatment. This annealing is done together with ~0.1 g Gd_2O_3 powder sealed in the same silica tube to supply an oxygen source. The strong diamagnetic signal demonstrates the bulk superconducting character in the GdFePO sample with the post-annealing treatment. In contrast, no diamagnetic signal could be detected from the GdFePO product without this post-annealing treatment, although a decrease of susceptibility value along with decreasing temperature is observed. Fig. 2(b) shows the Meissner shielding volume as a function of temperature, confirming the bulk superconductivity. The superconducting (SC) volume fraction is estimated based on the magnetization, the geometric volume of the specimen and the applied magnetic field. Because the AC susceptibility is measured in our experiment, a dissipation peak (χ'') can be found (not shown here), which could be used to reconfirm the transition temperature. The SC volume fraction in the measured sample reaches as high as more than 50% below 5 K and more than 90% below 2 K, confirming the high quality of our superconducting sample, which is in consistent with the SEM observation. Fig. 2(c) shows the temperature dependence of the resistivity measured from the GdFePO samples with and without post-annealing, respectively, under an applied field of 5 Oe. Zero resistivity is observed from the GaPePO sample with the post-annealing but not from the GaPePO sample without the post-annealing treatment. The superconducting critical temperature (T_c) as defined by the onset point of the resistivity is around 6.1 K.

Most surprisingly, an anomaly from the curve of magnetic susceptibility is found between the temperature ranges of 210–260 K, which might be associated with an antiferromagnetic (AF) transition based on the following experiments (Fig. 2(a)). From ~300 K, the magnetic susceptibility increases almost linearly with decreasing the temperature, but roughly below ~260 K for GdFePO with the post-annealing and ~210 K for GdFePO without the post-annealing, the magnetic susceptibility drops steeply. After the post-annealing treatment, the overall susceptibility decreases and the ~260 K anomaly shifts to ~210 K and becomes less pronounced. While the temperature approaches 6.1 K, a superconducting transition occurs. To further confirm this AF transition results actually from the bulk phase itself but not from other magnetic impurity. Magnetic hysteresis loops for GdFePO sample with the post-annealing treatment is measured under strong fields and at low temperatures, as shown

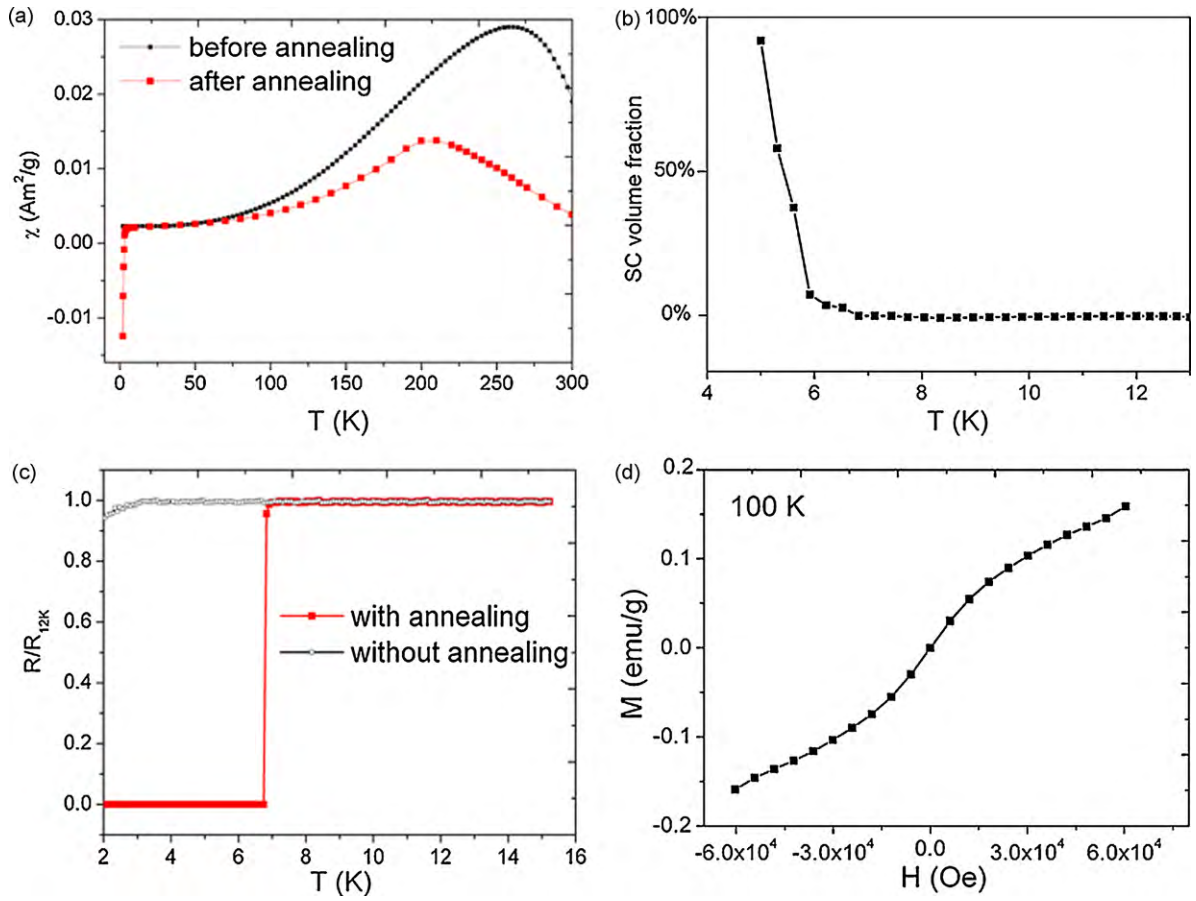

Fig. 2. (a) AC magnetic susceptibility measured from GdFePO before and after annealing as a function of temperature, respectively. The measurement was performed under an applied field of H_{AC} = 1 Oe. (b) Superconducting (SC) volume fraction in the GdFePO sample. (c) Temperature dependence of the resistance for GdFePO sample before and after annealing, showing zero resistance property at ~6.7 K in the later case. (d) A M–H hysteresis loop measured from GdFePO at 100 K.

in Fig. 2(d). This field dependence of the magnetic hysteresis shows a linear feature, but shows no loop feature. Even if a fine scanning speed is used in an applied magnetic field range of <50 Oe, no hysteresis loop can be observed. As the temperature is raised up to 250 K, saturated behavior can somewhat be observed after the magnetic field exceeds ~3000 Oe. It is indicated that a transition from ferromagnetic to antiferromagnetic happens. The above evidences strongly indicate that the anomaly at ~260 K observed from the *M–T* curve results actually from GdFePO itself but not from the magnetic impurity. From the XRD pattern and SEM image, it also can be known that the crystalline quality of our product is quite high. No trace of residual impurity can be detected from our detail electron microscopy and X-ray diffraction examinations. To investigate the influence of this AF order on the scattering blocking effect of the transporting electrons, dependence of resistivity on temperature is measured at high temperature such as the range of 200–300 K. No anomaly could be observed between 210 and 260 K. Hence, it is indicated that the resistivity originated from itinerant electrons. It is different from the conventional superconducting mechanism of cuprate oxide, which is based on Mott insulator doped by transporting carrier.

In order to research the annealing effect on the superconductivity occurrence, the crystalline defects in GdFePO was emphasized. Diffraction contrast imaging was performed using a Tecnai F20 TEM. Therefore, the correlation between the GdFePO superconductivity and the post-annealing was well established. Fig. 3(a) and (b) shows the microstructures of GdFePO with and without the post-annealing treatment, respectively. Dark-field image using weak beam $\vec{g} = 001$ was recorded to observe the crystalline defects. For instance, one grain was embedded inside several groups of parallel dislocations. Most of the grain boundaries are trapped inside the dislocation networks. From the corresponding electron diffraction pattern as shown in Fig. 3(d), these dislocation lines are well stacked along (0 0 1) crystalline planes of GdFePO. These TEM evidences reveal the presence of parallel dislocation matrix residing in the *a–b* crystal plane. Such high density of dislocations results in apparent structural distortions and strain field in the vicinal areas, and therefore becomes a type of strong scattering centre for the superconducting electrons. So huge amount of dislocation lines might pin the transporting electrons and destroy superconducting states. In contrast, only a little amount of dislocations could be detected from the GdFePO product after the post-annealing. Crystalline grains become more homogeneous via the cultivation. Besides, the grain integrality was improved and the amount of defects is much reduced. Hence, the dislocation density depends essentially on the post-annealing treatment. The post-annealing might make the original GdFePO to be $GdFePO_{1-x}$, which is an off-stoichiometry pnictides, as similar as described in Ref. [14].

It is well known that superconductivity inside FeAs system can occur via suppressing spin density wave (SDW) order. However, AF order has not been found inside FeP system. LaFeAsO is a poor metal and exhibit Pauli paramagnetism. Anomalies in spin density wave (ADW), specific heat and magnetic susceptibility play a key role in the superconductivity of FeAs systems. Using phosphor to replace arsenic, the competition between superconducting order and spin order was supposed to be adjusted due to the different bonding length between Fe–P and Fe–As. Moreover, the scattering and overlap between electron clouds were changed. Although the

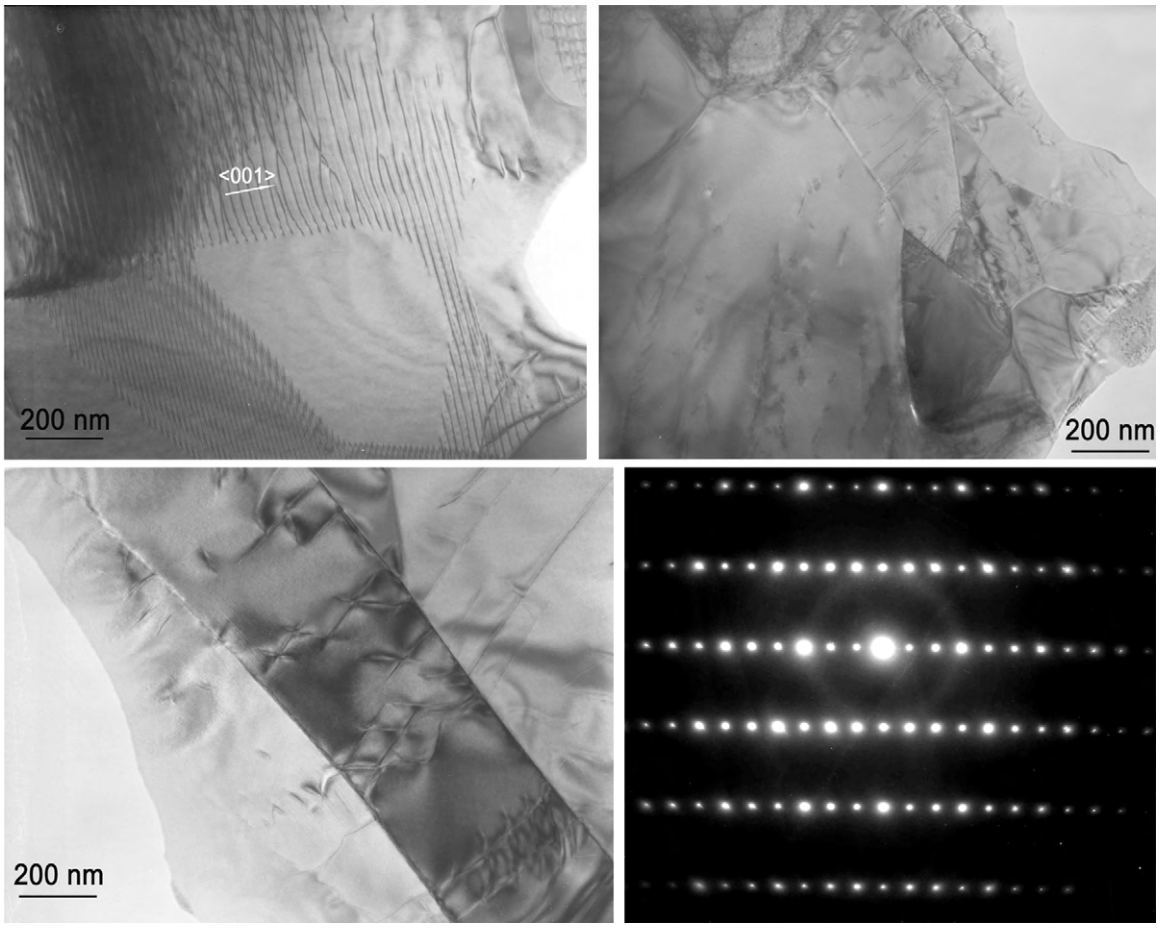

Fig. 3. (1) A TEM image of a typical region of GdFePO crystals before annealing. (b) and (c) recorded from GdFePO crystals after annealing, showing the reduction of the dislocation densities. (d) An electron diffraction pattern taken from the area as shown in (a).

origin of AF order from GdFePO is still unclear, it is suggested that the post-annealing suppress AF order and induce superconductivity based on our above analysis and experimental data.

4. Conclusions

In conclusion, a new pnictide oxide GdFePO superconductor has been synthesized by a combined solid-state reaction and arc melting method. The coexistence of antiferromagnetism order and superconductivity order in GdFePO is observed. The competing orders could be tuned via an important post-annealing treatment done after the synthesis. The significance of our finding is that the AF transition was found from FeP system and that a post-annealing could effectively reduce the dislocation density, which has a blocking influence on the superconductivity.

Acknowledgements

This work is supported by the National Natural Foundation of China (Nos. 50872145 and 10776037) and the Ministry of Science and Technology of China (973 Project Nos. 2007CB936301 and 2009CB930803). The authors are grateful to the “Shu Guang” project supported by Shanghai Municipal Education Commission and Shanghai Education Development Foundation (09SG01) and No. 9140C4403090902 (Key Lab., Project). We thank Prof. H.H. Wen for useful instructions.

References

[1] Y. Kamihara, T. Watanabe, M. Hirano, H. Hosono, J. Am. Chem. Soc. 130 (2008) 3296.
[2] X.Q. Wang, Q.Q. Liu, Y.X. Lv, W.B. Gao, L.X. Yang, R.C. Yu, F.Y. Li, C.Q. Jin, Solid State Commun. 148 (2008) 538.
[3] M. Rotter, M. Tegel, D. Johrendt, Phys. Rev. Lett. 101 (2008) 107006.
[4] Y. Kamihara, H. Hiramatsu, M. Hirano, R. Kawamura, H. Yanagi, T. Kamiya, H. Hosono, J. Am. Chem. Soc. 128 (2006) 10012.
[5] S. Matsuishi, Y. Inoue, T. Nomura, H. Yanagi, M. Hirano, H. Hosono, J. Am. Chem. Soc. 130 (2008) 14428.
[6] J. Janaki, T. Kumary, A. Mani, S. Kalavathi, G.V.R. Reddy, G.V. Rao, A. Bharathi, J. Alloys Compd. 486 (2009) 37.
[7] H.H. Wen, G. Mu, L. Fang, H. Yang, X. Zhu, Europhys. Lett. 82 (2008) 17009.
[8] B.I. Zimmer, W. Jeitschko, J.H. Albering, R. Claum, M. Reehuis, J. Alloys Compd. 229 (1995) 238.
[9] G.F. Chen, Z. Li, D. Wu, G. Li, W.Z. Hu, J. Dong, P. Zheng, J.L. Luo, N.L. Wang, Phys. Rev. Lett. 100 (2008) 247002.
[10] R.E. Baumbach, J.J. Hamlin, L. Shu, D.A. Zocco, N.M. Crisosto, M.B. Maple, New J. Phys. 11 (2009), 025018.
[11] L. Ortenzi, E. Cappelluti, L. Benfatto, L. Pietronero, Phys. Rev. Lett. 103 (2009) 046404.
[12] T. Yildirim, Phys. Rev. Lett. 101 (2008) 057010.
[13] C.Y. liang, R.C. Che, H.X. Yang, H.F. Tian, R.J. Xiao, J.B. Lu, R. Li, J.Q. Li, Supercond. Sci. Technol. 20 (2007) 687.
[14] R.C. Che, R.J. Xiao, C.Y. liang, H.X. Yang, C. Ms, H.L. Shi, J.Q. Li, Phys. Rev. B 77 (2008) 184518.
[15] A. Blachowski, K. Ruebenbauer, J. Żukrowski, J. Przewoźnik, K. Wojciechowski, Z.M. Stadnik, J. Alloys Compd. 494 (2010) 1.
[16] X.Z. Jin, T. Watanabe, K. Takase, Y. Takano, J. Alloys Compd. 488 (2009) L14.
[17] J. Janaki, T.G. Kumary, A. Mani, S. Kalavathi, G.V.R. Reddy, G.V.N. Rao, A. Bharathi, J. Alloys Compd. 486 (2009) 37.
[18] P. Cheng, B. Shen, J.P. Hu, H.H. Wen, Phys. Rev. B 81 (2010) 174529.